Diastereoselective formation of luminescent dinuclear lanthanide(III) helicates with enantiomerically pure tartaric acid derived bis(β-diketonate) ligands†

Markus Albrecht,*[a] Sören Schmid,[a] Sabrina Dehn,[a] Claudia Wickleder,[b] Shuang Zhang,[b] Andrew P. Bassett,[c] Zoe Pikramenou[c] and Roland Fröhlich[d]

Received (in Montpellier, France) 3rd April 2007, Accepted 24th May 2007
First published as an Advance Article on the web 22nd June 2007
DOI: 10.1039/b705090a

The chiral tartaric acid derived bis(β-diketonate) ligands **1**–**3**-H_2 diastereoselectively form dinuclear triple-stranded helicates with a series of lanthanide(III) ions (La, Ce, Pr, Nd, Sm, Eu, Gd, Tb, Dy, Ho, Er, Yb), which bind water molecules as additional co-ligands. In the cases of europium(III) and terbium(III) ions, bright red or green luminescence is observed, respectively. Hereby the energy transfer from the ligand to the metal is most effective with the bromophenyl-substituted ligand **3**-H_2. Reaction of **3**-H_2 with europium(III) in a 4 : 2 ratio results in a highly luminescent quadruple-stranded dinuclear complex $[\mathbf{3}_4Eu_2]^{2-}$.

Introduction

Due to their special photophysical, magnetic and electronic properties lanthanide metal complexes play an important role in recent coordination chemistry.[1] Potential applications of the compounds are found in the fields of diagnostics, peptide labeling, and inorganic phosphors. Many coordination compounds have been investigated due to the special luminescence properties of the different lanthanide ions.[2] Because $4f^n \leftrightarrow 4f^n$ transitions are forbidden due to the parity selection rule, emission after direct excitation into the 4f states is rather weak. Therefore, an energy transfer (ET) from a ligand aromatic unit to the metal has to occur in order to improve the emission intensity.[3] This principle, which is described as an "antenna effect", is shown in Fig. 1 for a europium(III) complex. In order to get bright emission, the energy transfer has to be highly effective.[4] In most cases a triplet pathway is involved, where the energy is transferred from the ligand centered triplet state T_1. In general, the choice of the ligand is therefore of importance for the efficiency of the emission and in particular β-diketonate ligands are mostly excitable in the near UV range and, thus, well known, to form highly luminescent lanthanide(III) complexes.[5,6]

In our ongoing program on the chemistry of helicates[7] we became interested in the stereoselective preparation of enantiopure triple-stranded helicates.[8] Therefore, we synthesized an enantiomerically pure bis(β-diketonate) ligand and used it for the formation of triple-stranded dinuclear helicates with iron(III) or gallium(III) ions.[9] We realized that there is only one example of an enantiomerically pure triple-stranded dinuclear helicate with lanthanide ions[10] known in the literature,[11] although several mononuclear[12] or heteronuclear enantiopure lanthanide complexes were already described.[13]

Herein, we show that our bis(β-diketonate) ligands, which are obtained from (*R*,*R*)-tartaric acid, can be used for the formation of dinuclear triple-stranded (and quadruple-stranded) lanthanide complexes, which show promising strong red emission in the case of Eu(III) compounds and also strong green emission for Tb(III) compounds.

The substituents at the β-diketonate moiety are varied systematically (Me → Ph → 4-BrPh) to tune the efficiency of the energy transfer from the ligand to the metal ion.

Results and discussion

Ligand synthesis

The chiral bis(β-diketonate) ligands **1**–**3**-H_2 were prepared in a Claisen-type condensation reaction starting from the acetone

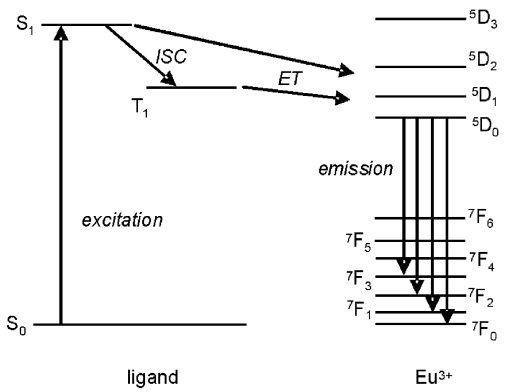

Fig. 1 Schematic representation of the energy transfer pathways in a Eu(III) complex (ISC = intersystem crossing).

[a] *Institut für Organische Chemie der RWTH-Aachen, Landoltweg 1, D-52074 Aachen, Germany. E-mail: markus.albrecht@oc.rwth-aachen.de; Fax: +49 241 80 92385*
[b] *Anorganische Chemie, Universität Siegen, 57068 Siegen, Germany*
[c] *School of Chemistry, The University of Birmingham, Edgbaston, UK B15 2TT*
[d] *Organisch-Chemisches Institut, Universität Münster, Corrensstrasse 40, 48149 Münster, Germany*

† Electronic supplementary information (ESI) available: Characterization data for complexes $\mathbf{2}_3M_2$ and $\mathbf{3}_3M_2$, ligand **3** emission/excitation spectra and data for ligand emission in complexes. See DOI: 10.1039/b705090a

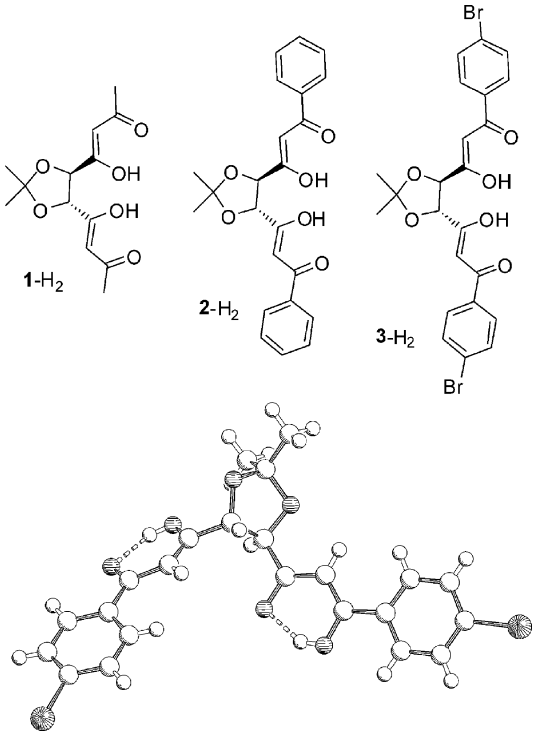

Fig. 2 Ligands **1**–**3**-H_2 and the solid state structure of **3**-H_2.

ketal of (*R*,*R*)-tartaric acid diethylester. This diester is reacted with acetone, acetophenone, or *p*-bromoacetophenone in the presence of sodium amide as base.[14]

The solid phase structure of **3**-H_2 is shown in Fig. 2. It is found, that the compound crystallizes in the bis(enol) form, as it is observed as the major component in the NMR spectrum of the ligand in chloroform.[9]

Preparation of dinuclear metal complexes

Dinuclear lanthanide(III) complexes are obtained by reaction of three equivalents of ligand **1**–**3**-H_2 with two equivalents of $LnCl_3$ (Ln = La, Ce, Pr, Nd, Sm, Eu, Gd, Tb, Dy, Ho, Er, Yb) and three equivalents of potassium carbonate in methanol. After overnight stirring, solvent is removed and the residue is extracted with isopropanol and insoluble material is filtered off. Isopropanol is removed *in vacuo* to obtain the dinuclear triple-stranded complexes (Scheme 1). The obtained compounds $\mathbf{L}_3Ln_2$ are listed in Table 1. For a representative MS spectrum see Fig. 3.

Table 1 lists the triple-stranded dinuclear lanthanide(III) complexes that are formed. Hereby, elemental analyses reveal that water molecules are always included in the material. From the analyses it is not clear if this water is bound to the lanthanide centers, if it is encapsulated in the complexes as observed in the crystal structure of the gallium compound $[(H_2O)\subset\{\mathbf{3}_3Ga_2\}]$, or if it is crystal-water. Some of the MS spectra indicate that two water molecules are tightly attached to the metals. For example, a peak corresponding to $[\mathbf{3}_3Sm_2(H_2O)_2]$ is observed at m/z = 2013 $[\mathbf{3}_3Sm_2(H_2O)_2Na]^+$. In the case of the lanthanum(III) compound, with large central metal ions, two water molecules are bound to each metal, m/z = 2023 $[\mathbf{3}_3La_2(H_2O)_4Na]^+$.[15]

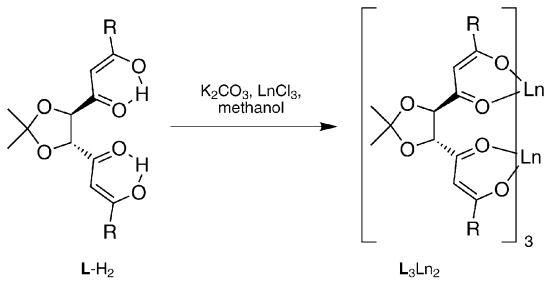

Scheme 1 Preparation of metal complexes $\mathbf{L}_3Ln_2$.

NMR measurements did not provide informative spectra. We detected resonances of neither a defined complex nor of the free ligand. This is probably due to a highly dynamic behavior of the complexes, which is not understood at the present time.

Solution CD spectroscopy of $\mathbf{3}_3Eu_2$, $\mathbf{3}_3Tb_2$, and $\mathbf{3}_3Ho_2$ was performed in dichloromethane (Fig. 4). Under those conditions, the free ligand **3**-H_2 leads to a positive Cotton effect at 300 nm and a negative one at 340 nm.[14] In the corresponding lanthanide(III) complexes, the ligand centered transitions are shifted to 325 (−) and 350 nm (+) with reversed Cotton effects. This indicates a different conformation of the free ligand compared to the ligand in the complex. On the other hand, $\mathbf{3}_3Ga_2$ shows a similar CD spectrum compared to the free ligand, which indicates a similar conformation of the ligand and its complexed form.[16]

Luminescence properties of $\mathbf{L}_3Ln_2$ (Ln = Eu, Tb, Ho, La)

Due to the dynamic behaviour of the compounds in solution, which was observed by NMR spectroscopy, luminescence investigations of the complexes were done in the solid phase.[17] In this form all compounds show strong red (Ln = Eu) or green (Ln = Tb, Ho) emission if irradiated by a UV lamp. For comparison, the excitation and emission spectra of the pure ligand **3**-H_2 were also recorded.

Complexes $\mathbf{1}_3Ln_2$ (Ln = Eu, Tb). Fig. 5 depicts the excitation and emission spectra of the complexes $\mathbf{1}_3Ln_2$ (Ln = Eu, Tb). In both cases two strong ligand excitation bands are observed in the excitation spectra by detection of the $^5D_0 \rightarrow {}^7F_2$ (Eu) and $^5D_4 \rightarrow {}^7F_6$ (Tb) transitions, respectively, of the lanthanide ions (Table S1, ESI†). They can be assigned to the singlet ligand transitions. For $\mathbf{1}_3Eu_2$ an additional shoulder is observed at about 400 nm. This observation clearly points to a ligand → metal ion energy transfer. The positions of the bands are comparable in both complexes (Table S1, ESI†), therefore the conformation of the aromatic units is assumed to be nearly the same. The relative intensities of the two bands show that the energy transfer from the high energy ligand state is more efficient than those from the low energy one in the complex $\mathbf{1}_3Tb_2$, while it is of comparable efficiency in $\mathbf{1}_3Eu_2$. In the case of the latter also, some relatively strong narrow peaks are detected in the excitation spectrum, which can be assigned to intra $^7F_0 \rightarrow {}^5D_J$ transitions of the Eu^{3+} ions. The respective transitions are not observed in the Tb complex although some

Table 1 Analytical data for lanthanide complexes of the bis(β-diketonate) ligands. The ESI MS spectra were sprayed from methanol or chloroform–methanol. The highest peak out of the isotope mixture is given. (Traces of NaCl are introduced during the sample preparation, which lead to the observation of Na adducts in the positive, and of Cl adducts in the negative detection mode)

	L = 1		**L = 2**		**L = 3**	
	Positive ESI MS	Analysis found for	Positive ESI MS	Analysis found for	Positive ESI MS	Analysis found for
$\mathbf{L}_3La_2$	1105 $[M + Na]^+$, 1083 $[M + H]^+$	$\mathbf{1}_3La_2 \cdot 4H_2O$	739 $[M + Na + H]^{2+}$	$\mathbf{2}_3La_2 \cdot 5H_2O$	2023 $[M + 4H_2O + Na]^+$	$\mathbf{3}_3La_2 \cdot 3H_2O$
$\mathbf{L}_3Ce_2$	1085 $[M + H]^+$	$\mathbf{1}_3Ce_2 \cdot 4H_2O$	1457 $[M + H]^+$	$\mathbf{2}_3Ce_2 \cdot 5H_2O$	988 $[M + 2Na]^{2+}$	$\mathbf{3}_3Ce_2 \cdot 3H_2O$
$\mathbf{L}_3Pr_2$	1109 $[M + Na]^+$, 1087 $[M + H]^+$	$\mathbf{1}_3Pr_2 \cdot 2H_2O$	1493 $[M + Cl]^-$[a]	$\mathbf{2}_3Pr_2 \cdot 2H_2O$	1967 $[M + H_2O + OH]^-$[a]	$\mathbf{3}_3Pr_2 \cdot 3H_2O$
$\mathbf{L}_3Nd_2$	1117 $[M + Na]^+$, 1095 $[M + H]^+$	$\mathbf{1}_3Nd_2 \cdot 5H_2O$	1465 $[M + H]^+$	$\mathbf{2}_3Nd_2 \cdot 2H_2O$	1995 $[M + H_2O + K]^+$	$\mathbf{3}_3Nd_2 \cdot 3H_2O$
$\mathbf{L}_3Sm_2$			1512 $[M + Cl]^-$[a]	$\mathbf{2}_3Sm_2 \cdot 3H_2O$	2013 $[M + 2H_2O + Na]^+$	$\mathbf{3}_3Sm_2 \cdot 5H_2O$
$\mathbf{L}_3Eu_2$	1131 $[M + Na]^+$, 1109 $[M + H]^+$	$\mathbf{1}_3Eu_2 \cdot 3H_2O$	1503 $[M + Na]^+$	$\mathbf{2}_3Eu_2 \cdot H_2O$	1977 $[M + Na]^+$	$\mathbf{3}_3Eu_2 \cdot 3H_2O$
$\mathbf{L}_3Gd_2$			1494 $[M + H]^+$	$\mathbf{2}_3Gd_2 \cdot 4H_2O$		
$\mathbf{L}_3Tb_2$	1145 $[M + Na]^+$, 1123 $[M + H]^+$	$\mathbf{1}_3Tb_2 \cdot 3H_2O$	1495 $[M + H]^+$	$\mathbf{2}_3Tb_2 \cdot 3H_2O$	2039 $[M + 2H_2O + Cl]^-$[a]	$\mathbf{3}_3Tb_2 \cdot 2H_2O$
$\mathbf{L}_3Dy_2$	1170 $[M + Na + H_2O]^+$, 1152 $[M + Na]^+$, 1131 $[M + H]^+$	$\mathbf{1}_3Dy_2 \cdot 2H_2O$	1502 $[M + H]^+$	$\mathbf{2}_3Dy_2 \cdot 3H_2O$	1975 $[M]^+$	$\mathbf{3}_3Dy_2 \cdot 2H_2O$
$\mathbf{L}_3Ho_2$	1134 $[M + H]^+$	$\mathbf{1}_3Ho_2 \cdot 2H_2O$	1507 $[M + H]^+$	$\mathbf{2}_3Ho_2 \cdot H_2O$	2016 $[M + 2H_2O]^+$	$\mathbf{3}_3Ho_2 \cdot 2H_2O$
$\mathbf{L}_3Er_2$			1511 $[M + H]^+$	$\mathbf{2}_3Er_2 \cdot 3H_2O$	2021 $[M + 2H_2O + H]^+$	$\mathbf{3}_3Er_2 \cdot 3H_2O$
$\mathbf{L}_3Yb_2$	1173 $[M + Na]^+$, 1151 $[M + H]^+$	$\mathbf{1}_3Yb_2 \cdot 3H_2O$	1523 $[M + H]^+$	$\mathbf{2}_3Yb_2 \cdot 2H_2O$	2056 $[M + 2H_2O + Na]^+$, 2037 $[M + H_2O + Na]^+$	$\mathbf{3}_3Yb_2 \cdot 3H_2O$

[a] Negative ESI MS.

4f → 4f transitions are located in the range of 300 to 450 nm (*e.g.* $^7F_6 \rightarrow {}^5L_{10}$ at about 370 nm).[17] Therefore, it can be assumed that the excitation process inside the ligands is stronger in $\mathbf{1}_3Tb_2$ than in the europium complex $\mathbf{1}_3Eu_2$ because the intra Tb excitations are too weak to be detected.

Emission spectra with ligand excitation of both complexes are also shown in Fig. 5. Narrow peaks are observed, which can be assigned to intra 4f → 4f transitions of the lanthanide ions ($^5D_0 \rightarrow {}^7F_J$ for $\mathbf{1}_3Eu_2$ and $^5D_4 \rightarrow {}^7F_J$ for $\mathbf{1}_3Tb_2$, respectively).[17] Even in high resolution no crystal field splitting is observed, probably due to line broadening by lattice effects or thermal vibrations. For the terbium(III) complex this may be due to the large number of Stark levels of the states with high *J* values, which is also obvious from the larger full width of half maximum (FWHM) of the $^5D_4 \rightarrow {}^7F_5$ emission compared to the Eu $^5D_0 \rightarrow {}^7F_2$ emission peak. In the case of $\mathbf{1}_3Eu_2$, however, detection of different crystal field levels can be expected even with room temperature measurements. This indicates the presence of more than one crystallographically different Eu site and, moreover, low point symmetries of these sites. The latter is also expected from the fact that the hypersensitive $^5D_0 \rightarrow {}^7F_2$ transition is much more intense than the magnetic dipole $^5D_0 \rightarrow {}^7F_1$ transition[18] ($I(^5D_0 \rightarrow {}^7F_2)/I(^5D_0 \rightarrow {}^7F_1) = 18$). Note that, in the case of the Tb complex $\mathbf{1}_3Tb_2$, the blue $^5D_3 \rightarrow {}^7F_J$ transitions, which are located at higher energies and which would result in a bluish white emission, are not observed in the present case. This can be explained by the high Tb^{3+} concentration, which may cause an efficient cross relaxation ($Tb(^5D_3) + Tb(^7F_6) \rightarrow Tb(^5D_4) + Tb(^7F_0)$) and leads to a high colour quality of the emission.[19]

In the emission spectrum of the Tb compound $\mathbf{1}_3Tb_2$ ligand emission is detected at about 400 nm, which, unfortunately, decreases the color quality of the emission. This is not observed for the Eu complex $\mathbf{1}_3Eu_2$. While the ligand → Eu energy transfer is complete in $\mathbf{1}_3Tb_2$, a part of the excitation energy is not transferred to the lanthanide ion. Because the structures of both complexes should be similar due to the comparable size of the lanthanide ions, the more efficient ET process for the Eu complex should be caused by the better energetic overlap of the ligand emission bands with the Eu excitation bands. Furthermore, the larger excitation probability of the Tb aromatic units compared to the Eu ones is also assumed to influence the ET process.

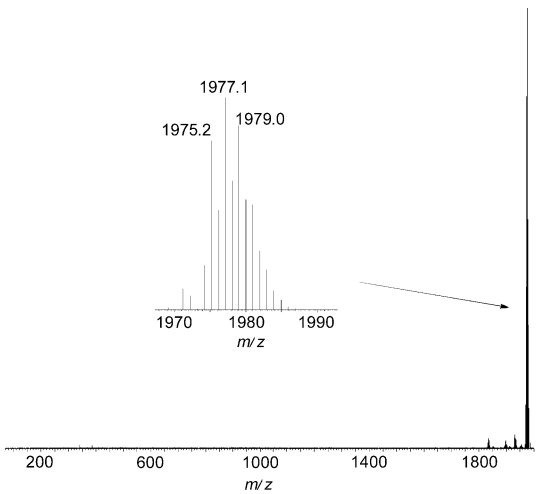

Fig. 3 ESI MS spectrum of $\mathbf{3}_3Eu_2$ sprayed from methanol. The inset shows the isotopic pattern of the peak at $m/z = 1977$ [$\mathbf{3}_3Eu_2Na$], which matches the calculated one.

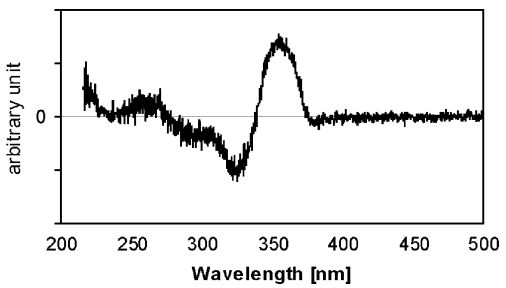

Fig. 4 CD spectra of $\mathbf{3}_3Tb_2$ measured in dichloromethane. The corresponding spectra of $\mathbf{3}_3Eu_2$, and $\mathbf{3}_3Ho_2$ are virtually identical.

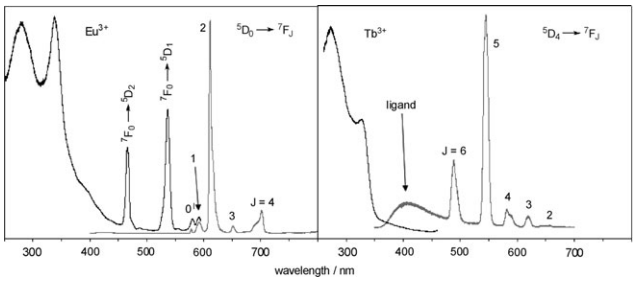

Fig. 5 Room temperature luminescence spectra of the complexes $\mathbf{1}_3Ln_2$ (left: Ln = Eu, λ_{em} = 610 nm, λ_{ex} = 340 nm; right: Ln = Tb, λ_{em} = 488 nm, λ_{ex} = 330 nm). Black line: excitation spectra, gray line: emission spectra.

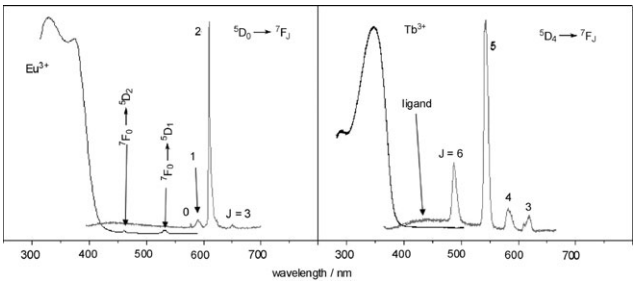

Fig. 7 Room temperature luminescence spectra of the complexes $\mathbf{3}_3Ln_2$ (left: Ln = Eu, λ_{em} = 610 nm, λ_{ex} = 375 nm; right: Ln = Tb, λ_{em} = 543 nm, λ_{ex} = 344 nm). Black line: excitation spectra, gray line: emission spectra.

Complexes $\mathbf{2}_3Ln_2$ (Ln = Eu, Tb). The emission and excitation spectra of the complexes $\mathbf{2}_3Ln_2$ (Eu, Tb) (Fig. 6) are different from the already described ones. However, they show, in general, again ligand → lanthanide ion ET activities. The ligand singlet excitation bands (Eu: 379 nm, Tb: 340 nm, ESI: Table S1†) are shifted to lower energy compared to the $\mathbf{1}_3Ln_2$ ones, as is expected due to the larger π system of the ligands. In this case the maxima of the bands of both complexes are quite different, which points to different solid phase structures. This is in agreement with the elemental analysis (Table 1) resulting in different compositions of the Eu and Tb complexes. Again, some intra 4f → 4f excitation peaks are detected for the Eu complex that are of lower relative intensity compared to those of $\mathbf{1}_3Eu_2$. This observation points to a larger transition probability of the aromatic unit in the case of $\mathbf{2}_3Ln_2$.

The emission spectra of $\mathbf{2}_3Ln_2$ show again the narrow $^5D_J \rightarrow {}^7F_J$ peaks of the lanthanide ions without resolution of the crystal field levels and a larger FWHM of the $^5D_4 \rightarrow {}^7F_5$ emission (Tb complex) compared to that of the $^5D_0 \rightarrow {}^7F_2$ emission (Eu complex). Also in this case, the large intensity ratio ($I(^5D_0 \rightarrow {}^7F_2)/I(^5D_0 \rightarrow {}^7F_1)$) points to low site symmetry. While the $S_1 \rightarrow S_0$ emission band is somewhat smaller for $\mathbf{2}_3Tb_2$ compared to $\mathbf{1}_3Tb_2$, the emission spectrum of $\mathbf{2}_3Eu_2$ includes a large respective emission band with a much higher intensity than the $^5D_0 \rightarrow {}^7F_J$ transitions. Therefore, the ET is of very low efficiency.

Complexes $\mathbf{3}_3Ln_2$ (Ln = Eu, Tb, Ho). Emission and excitation spectra of $\mathbf{3}_3Ln_2$ (Ln = Eu, Tb) are depicted in Fig. 7. The maxima of the ligand excitation bands are once again shifted to lower energy (ESI: Table S1†) and are different for both complexes, in agreement with the elemental analysis (Table 1). For $\mathbf{3}_3Tb_2$ they are located at higher energy compared to $\mathbf{3}_3Eu_2$, which points to a larger distortion of the planar π system in this complex. The $^7F_0 \rightarrow {}^5D_J$ transitions of the Eu complex are of very weak intensity and are not detectable in the Tb complex.

The emission spectra show identical $^5D_J \rightarrow {}^7F_J$ transitions of the lanthanide ions, which are already described for the other complexes. Again, their shape and intensity distribution lead to the assumption of several lanthanide sites of low symmetry. In the present case the ligand emission bands are extremely weak, showing a very efficient ET process for both complexes. Note that this fact, together with the large intensity of the $^5D_0 \rightarrow {}^7F_2$ transition, lead to a very high color quality, especially of the emission of $\mathbf{3}_3Eu_2$.

In conclusion, the complexes $\mathbf{3}_3Eu_2$ and $\mathbf{3}_3Tb_2$ yielded the most excellent results of all investigated compounds due to their high ET efficiency and the high ligand excitation probability. Also, the emission intensity observed with the naked eye is by far the highest for these compounds and extremely bright. The high ligand band/lanthanide line ratios in the excitation spectra demonstrate the high lanthanide emission intensity after ligand excitation and, thus, the large ET efficiency.

$\mathbf{3}_3Ho_2$ excitation and emission spectra are depicted in Fig. 8. The ligand excitation band peaks at about 340 nm, at comparable energy to the Tb^{3+} complex but at higher energy compared to the Eu^{3+} one. This is in agreement with the elemental analysis, which gives identical compositions for $\mathbf{3}_3Ho_2$ and $\mathbf{3}_3Tb_2$ but not for $\mathbf{3}_3Eu_2$ (Table 1). The excitation transitions inside the Ho 4f shell are very weak compared to those of the ligand, pointing to a strong excitation efficiency of the latter.

The Ho $^{2S+1}L_J \rightarrow {}^5I_J$ peaks observable in the emission spectrum are relatively broad due to the large J values of the states included and, moreover, due to the crowded energy level diagram of Ho. The latter causes also a manifold of emission transitions and, thus, rather low emission intensity in the visible region. Additionally, a broad emission band is detected in the emission spectrum, which can be assigned to a ligand transition. This indicates poor energy transfer efficiency for $\mathbf{3}_3Ho_2$ in contrast to the complexes $\mathbf{3}_3Tb_2$ and $\mathbf{3}_3Eu_2$.

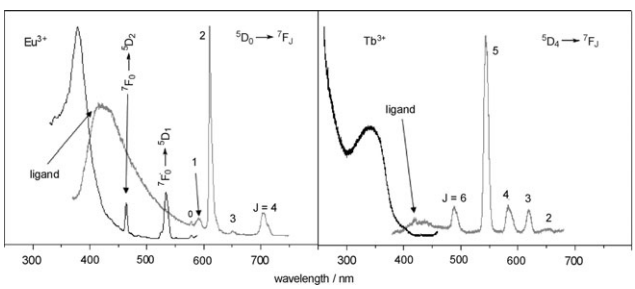

Fig. 6 Room temperature luminescence spectra of the complexes $\mathbf{2}_3Ln_2$ (left: Ln = Eu, λ_{em} = 610 nm, λ_{ex} = 350 nm; right: Ln = Tb, λ_{em} = 490 nm, λ_{ex} = 350 nm). Black line: excitation spectra, gray line: emission spectra.

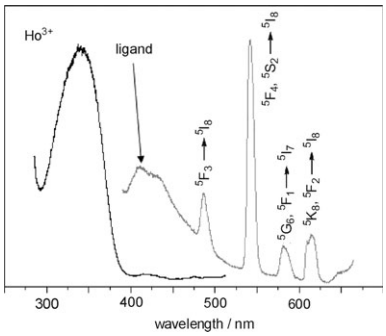

Fig. 8 Room temperature luminescence spectra of $\mathbf{3}_3Ho_2$, λ_{em} = 545 nm, λ_{ex} = 356 nm. Black line: excitation spectrum, gray line: emission spectrum.

Complexes L_3La_2. For the investigation of the energetic positions of the ligand triplet states we also performed emission measurements of the complexes $\mathbf{L}_3La_2$ (Fig. 9). Due to the absence of 4f states, no ligand–lanthanide ion energy can occur in these cases and emission from the ligand triplet states is detected as very broad bands in the near UV or visible region with maxima at about 505 nm ($\mathbf{1}_3La_2$), 410 nm ($\mathbf{2}_3La_2$), and 480 nm ($\mathbf{3}_3La_2$), respectively. The small peaks at 612 nm are caused by small amounts of Eu^{3+} ions. The shape and position of the band observed for $\mathbf{2}_3La_2$ is very similar to the ligand emission of $\mathbf{2}_3Eu_2$ (Fig. 6). In contrast, the bands of $\mathbf{1}_3La_2$ and $\mathbf{3}_3La_2$ are remarkably red-shifted compared to those of $\mathbf{L}_3Ln_2$ (**L** = **1**, **3**, Ln = Eu, Tb, Ho). This points to similar structures in the former cases but to a different conformation of the ligand in the latter. In general, due to the broadness of the ligand triplet bands, an overlap with several $4f^n$ lanthanide excitation peaks occurs so that efficient energy transfer is possible.

Ligand 3-H_2. For comparison, luminescence spectra of the ligand **3**-H_2 in the solid state were recorded (ESI: Fig. S1†). Several transitions in the excitation spectrum, as well as in the emission spectrum, are detected, showing a raw mirror image of the two spectra. The maxima are at 409 and 494 nm, respectively, with a large red-shift compared to those observed in the spectra of the respective complexes. This can be explained by the fact that the ligand units in the complexes are much more distorted from the planar geometry compared to the solid state structure of the free ligands.

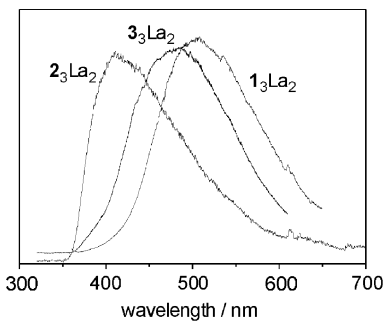

Fig. 9 Room temperature emission spectra of $\mathbf{3}_3La_2$.

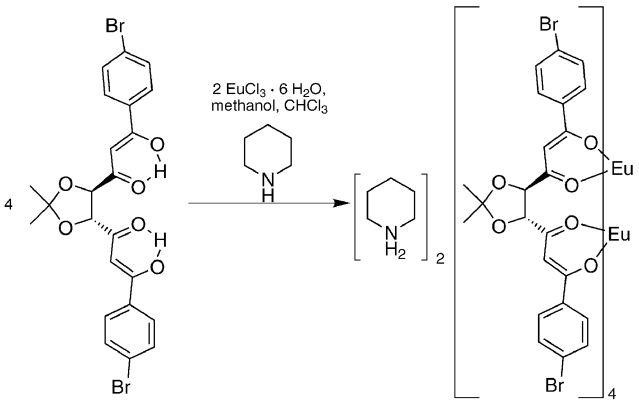

Scheme 2

Preparation and photophysical properties of $[H\text{-pip}]_2[\mathbf{3}_4Eu_2]$. In analogy to earlier work,[5] we wanted to investigate if the chiral bis(β-diketone) ligands are able to form enantiomerically pure quadruple-stranded helicate-type complexes. Therefore, ligand **3**-H_2 (4 equiv.) and $EuCl_3 \cdot 6H_2O$ were reacted in chloroform–methanol in the presence of piperidine (Scheme 2). A highly luminescent creamy powder was obtained.

ESI MS showed a peak in the negative mode at m/z = 2527 $[\mathbf{3}_4Eu_2 + Na]^-$ and in the positive mode at m/z = 2507 $[\mathbf{3}_4Eu_2 + 3H]^+$, revealing the presence of a 4 : 2 ligand : metal complex.

Excitation at λ = 337 nm of a solid powder sample of the product resulted in a strong luminescence spectrum, which showed the characteristic europium(III) emission bands of the $^5D_0 \rightarrow {}^7F_J$ transitions (Fig. 10). The pattern of the Eu(III) emission peaks, with a dominating $^5D_0 \rightarrow {}^7F_2$ transition, is in agreement with a high degree of symmetry of this complex as compared with the tris $\mathbf{3}_3$-Eu_2 complex.[20] In the latter, solvent coordination in the vacant sites reduces the overall symmetry of the complex. The excitation spectrum of the powder sample λ_{em} = 611 nm shows an absorption profile with a maximum at around 340 nm, in agreement with that of the UV-Vis absorption spectrum, which confirms ligand-sensitized luminescence.

By dissolving the powder of $[H\text{-pip}]_2[\mathbf{3}_4Eu_2]$ in DMF and examining the emission spectrum, it was observed that the line

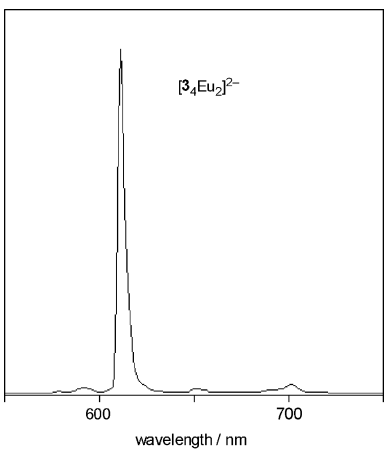

Fig. 10 Emission spectrum of a powder sample of $(H\text{-pip})_2[\mathbf{3}_4Eu_2]$ at 295 K, λ_{ex} = 337 nm.

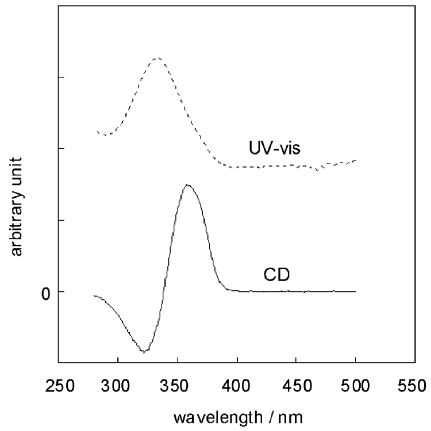

Fig. 11 Circular dichroism spectrum of a solution of (H-pip)$_2$[**3**$_4$Eu$_2$] in DMF. The UV-vis spectrum of the same solution is also presented (--).

pattern is characteristic of the tris complex, **3**$_3$Eu$_2$, indicating that conversion of the tris to the tetrakis complex is taking place in solution as was observed previously in the case of a bis(diketonate) ligand with a 1,3-phenyl spacer.[5] The UV-Vis spectrum of the complex in DMF shows a strong absorption band centred at 337 nm (ε = 190 000 M^{-1} cm^{-1}), corresponding to the $\pi \rightarrow \pi^*$ ligand transition. The quantum yield of the complex in DMF was estimated to be 10% using Ru(bpy)$_3$Cl$_2$ as external reference. The luminescence lifetime of the powder was measured for the $^5D_0$ excited state to be 0.25 ms, in contrast with the DMF solution where it was found to be 0.5 ms. The tris-complex [**3**$_3$Eu$_2$], prepared independently, shows the same lifetime of 0.5 ms in DMF solution. Powders of the tris-complex [**3**$_3$Eu$_2$] show a lifetime of 0.1 ms, however, the shorter lifetime as compared with the powder of the tetrakis-complex may be due to coordination of solvent molecules, which can provide an additional quenching pathway, and it cannot be directly compared with the tetrakis powder.

The circular dichroism spectra of solutions of (H-pip)$_2$-[**3**$_4$Eu$_2$] (Fig. 11) and **3** in DMF show a weak signal in the case of the ligand and a much stronger signal (negative Cotton effect) in the case of the complex, confirming the chiral nature of the helicate. The triple-stranded complex **3**$_3$Eu$_2$ shows a CD spectrum in dichloromethane that looks virtually the same. However, due to missing data for comparison, we cannot decide which configuration is present at the metal center.

Conclusions

Herein we presented the coordination chemistry of chiral bis(β-diketonate) ligands **1**–**3**-H$_2$ towards lanthanide(III) ions. A series of triple-stranded helicate-type complexes (**1**–**3**)$_3$Ln$_2$ was thus obtained. Elemental analysis as well as mass spectrometry indicates that vacant coordination sites at the metals can be filled by coordination of water. The europium(III) as well as terbium(III) complexes show typical luminescence behaviour in the solid state. Hereby the efficiency of the energy transfer between ligand and metal highly depends on the substituents at the terminus of the complex. The complexes (**3**$_3$Ln$_2$, Ln = Ho, Eu) with 4-BrPh as ligands yielded very high emission intensites of high color quality due to the strong ligand → lanthanide ion energy transfer processes with better luminescence properties compared to the complexes with ligands **1**-H$_2$ and **2**-H$_2$. In contrast, the luminescence behaviour of **3**$_3$Ho$_2$ is very poor. In addition, we presented the formation of a quadruple-stranded dinuclear europium(III) complex[21] that also shows interesting luminescence properties. Investigation of those in solution indicates that here an equilibrium between the quadruple- and the triple-stranded system is present.

Further studies will be performed, in which the substituents and the central spacer of the ligand will be varied in order to further influence the sensitization of the metal centers through the ligand. In addition, we are trying to prepare heterodinuclear complexes, which should be able to show some additional energy transfer between the metal centers.

Experimental

NMR spectra were recorded on a Varian Mercury 300, or Inova 400 spectrometer. FT-IR spectra were recorded by diffuse reflection (KBr) on a Bruker IFS spectrometer. Mass spectra (EI, 70 eV; FAB with 3-NBA as matrix) were taken on a Finnigan MAT 90, 95, or 212 spectrometer. ESI MS measurements were performed on a LCQ Deca XP Plus mass spectrometer and were sprayed from methanol or methanol–chloroform at concentrations of approximately 100 μM. UV-Vis spectra were recorded on a Perkin Elmer lambda2 spectrometer. Elemental analyses were obtained with a Heraeus CHN-O-Rapid analyzer. Melting points: Büchi B-540 (uncorrected).

Photoluminescence measurements on solid samples at room temperature were recorded on a Jobin-Yvon fluorescence spectrometer (Fluorolog 3) equipped with two 0.22 m double monochromators (SPEX, 1680) and a 450 W xenon lamp. The emission spectra were corrected for photomultiplier sensitivity, the excitation spectra for lamp intensity and both for the transmission of the monochromators.

Luminescence emission and excitation spectra for the tetrakis Eu(III) complex were recorded on a Photon Technology International (PTI) QM-1 emission spectrometer. Emission spectra were corrected for photomultiplier tube response. Lifetime measurements were carried out using a nanosecond Nd-YAG laser (Continuum, Surelite II) as the excitation source in an experimental set-up previously described (the experimental errors of the lifetimes are 15%).[22]

General procedure for the synthesis of **1**$_3$M$_2$ (M = La, Ce, Pr, Nd, Eu, Tb, Dy, Ho, Yb)

3*R*,4*R*-Bis(1,3-butandione)2,2-dimethyldioxolane **1**-H$_2$ (50 mg, 0.185 mmol) and potassium carbonate (25.6 mg, 0.185 mmol) are dissolved in 30 ml of methanol. After addition of 0.123 mmol lanthanide(III) chloride, the solution is stirred overnight at room temperature. The residue is dissolved in isopropanol and precipitates are filtered off. Solvent is removed *in vacuo* to obtain solid materials.

1$_3$**La**$_2$**.** Yield: 67 mg (0.058 mmol, 94%); IR (KBr): $\tilde{\nu}$ (cm^{-1}) = 2987, 2932, 1605, 1512, 1413, 1254, 1156, 1087, 1018, 929,

867, 789, 543; UV (EtOH): λ_{max} (nm) = 315 (sh), 297; positive ESI MS: m/z = 1105 $[M + Na]^+$, 1083 $[M + H]^+$; analysis calcd for $C_{39}H_{48}O_{18}La_2 \cdot 4H_2O$ (1154.67): C 40.57, H 4.89; found: C 40.47, H 4.86%.

1_3Ce_2. Yield: 67 mg (0.058 mmol, 94%.); IR (KBr): $\tilde{\nu}$ (cm^{-1}) = 2986, 2932, 1601, 1511, 1404, 1259, 1157, 1089, 1019, 867, 793, 532; UV (EtOH): λ_{max} (nm) = 316 (sh), 295; positive ESI MS: m/z = 1085 $[M + H]^+$, 1125 $[M + H_2O + Na]^+$; analysis calcd for $C_{39}H_{48}O_{18}Ce_2 \cdot 4H_2O$ (1157.10): C 40.48, H 4.88; found: C 40.63, H 4.94%.

1_3Pr_2. Yield: 66 mg (0.059 mmol, 95%); IR (KBr): $\tilde{\nu}$ (cm^{-1}) = 2987, 2931, 1602, 1511, 1411, 1257, 1212, 1154, 1089, 958, 930, 865, 791, 547; UV (EtOH): λ_{max} (nm) = 314 (sh), 296; positive ESI MS: m/z = 1109 $[M + Na]^+$, 1087 $[M + H]^+$; analysis calcd for $C_{39}H_{48}O_{18}Pr_2 \cdot 2H_2O$ (1122.65): C 41.73, H 4.67; found: C 41.56, H 5.05%.

1_3Nd_2. Yield: 67 mg (0.057 mmol, 92%); IR (KBr): $\tilde{\nu}$ (cm^{-1}) = 2988, 2934, 1604, 1511, 1413, 1256, 1212, 1157, 1088, 930, 866, 790, 550; UV (EtOH): λ_{max} (nm) = 313 (sh), 295; positive ESI MS: m/z = 1117 $[M + Na]^+$, 1095 $[M + H]^+$; analysis calcd for $C_{39}H_{48}O_{18}Nd_2 \cdot 5H_2O$ (1183.36): C 39.50, H 4.94; found: C 39.31, H 4.59%.

1_3Eu_2. Yield: 68 mg (0.058 mmol, 95%); IR (KBr): $\tilde{\nu}$ (cm^{-1}) = 2985, 2936, 1743, 1678, 1605, 1512, 1440, 1412, 1322, 1243, 1091, 866, 773; UV (EtOH): λ_{max} (nm) = 315 (sh), 291; positive ESI MS (ESI): m/z = 1131 $[M + Na]^+$, 1109 $[M + H]^+$; analysis calcd for $C_{39}H_{48}O_{18}Eu_2 \cdot 3H_2O$ (1162.77): C 40.29, H 4.68; found: C 40.29, H 4.74%.

1_3Tb_2. Yield: 69 mg (0.059 mmol, 95%); IR (KBr): $\tilde{\nu}$ (cm^{-1}) = 2988, 2936, 1604, 1513, 1415, 1259, 1212, 1157, 1092, 935, 867; UV (EtOH): λ_{max} (nm) = 311 (sh), 291; positive ESI MS: m/z = 1145 $[M + Na]^+$, 1123 $[M + H]^+$; negative ESI MS: m/z = 1157 $[M + Cl]^-$; analysis calcd for $C_{39}H_{48}O_{18}Tb_2 \cdot 3H_2O$ (1176.70): C 39.81, H 4.63; found: C 39.65, H 4.95%.

1_3Dy_2. Yield: 70 mg (0.060 mmol, 99%); IR (KBr): $\tilde{\nu}$ (cm^{-1}) = 2986, 2936, 1609, 1515, 1416, 1259, 1214, 1158, 1091, 1020, 935, 868, 793, 545; UV (EtOH): λ_{max} (nm) = 312 (sh), 292; positive ESI MS: m/z = 1170 $[M + H_2O + Na]^+$, 1152 $[M + Na]^+$, 1131 $[M + H]^+$; analysis calcd for $C_{39}H_{48}O_{18}Dy_2 \cdot 2H_2O$ (1165.83): C 40.18, H 4.50; found: C 40.01, H 4.87%.

1_3Ho_2. Yield: 70 mg (0.060 mmol, 99%); IR (KBr): $\tilde{\nu}$ (cm^{-1}) = 2988, 2935, 1607, 1514, 1415, 1259, 1213, 1157, 1092, 935, 868, 790; UV (EtOH): λ_{max} (nm) = 312 (sh), 292; positive ESI MS: m/z = 1134 $[M + H]^+$; analysis calcd for $C_{39}H_{48}O_{18}Ho_2 \cdot 2H_2O$ (1170.69): C 40.01, H 4.48; found: C 40.39, H 4.84%.

1_3Yb_2. Yield: 71 mg (0.059 mmol, 96%); IR (KBr): $\tilde{\nu}$ (cm^{-1}) = 2988, 2933, 1611, 1515, 1418, 1261, 1213, 1158, 1091, 1021, 936, 848, 797; UV (EtOH): λ_{max} (nm) = 311 (sh), 290; positive ESI MS (ESI): m/z = 1173 $[M + Na]^+$, 1151 $[M + H]^+$; analysis calcd for $C_{39}H_{48}O_{18}Yb_2 \cdot 3H_2O$ (1204.93): C 38.88, H 4.52; found: C 38.88, H 4.42%.

2_3M_2 and 3_3M_2 (M = La, Ce, Pr, Nd, Sm, Eu, Gd, Tb, Dy, Ho, Er, Yb)

Complexes of ligands **2**-H_2 and **3**-H_2 were prepared as described before.

[H-pip]$_2$[3_4Eu_2]

To a solution of $EuCl_3 \cdot 6H_2O$ (0.01 g, 0.027 mmol) in MeOH (3 ml), a solution of **3**-H_2 (0.03 g, 0.055 mmol) in $CHCl_3$ (3 ml) was added. Addition of 0.1 cm^3 of piperidine (pip) to this solution resulted in the immediate formation of a creamy precipitate, which was filtered, washed with MeOH and $CHCl_3$ and dried under vacuum (0.025 g, 68% yield). Negative ESI MS: m/z = 2527 $[M - 2(H\text{-pip}) + Na]^-$; positive ESI-MS: m/z = 2506 $[M - 2(H\text{-pip}) + 3H]^+$.

X-Ray crystal structure analysis for 3-H_2

Formula $C_{23}H_{20}Br_2O_6$, M = 552.21, colorless crystal 0.50 × 0.20 × 0.03 mm, a = 5.691(1), b = 9.359(1), c = 41.058(1) Å, V = 2186.8(5) $Å^3$, ρ_{calc} = 1.677 g cm^{-3}, μ = 3.745 mm^{-1}, empirical absorption correction ($0.256 \leq T \leq 0.896$), Z = 4, orthorhombic, space group $P2_12_12_1$ (no. 19), λ = 0.71073 Å, T = 223 K, ω and ϕ scans, 11822 reflections collected ($\pm h$, $\pm k$, $\pm l$), $[(\sin\theta)/\lambda]$ = 0.67 $Å^{-1}$, 5022 independent (R_{int} = 0.045) and 3682 observed reflections [$I \geq 2\sigma(I)$], 284 refined parameters, R = 0.042, wR^2 = 0.090, Flack parameter 0.001(10), max. residual electron density 0.48 (−0.67) e $Å^{-3}$, hydrogen atoms are calculated and refined riding. Data set was collected with a Nonius KappaCCD diffractometer, equipped with a rotating anode generator. Programs used: data collection COLLECT (Nonius BV, 1998), data reduction Denzo-SMN,[23] absorption correction Denzo,[24] structure solution SHELXS-97,[25] structure refinement SHELXL-97[25], graphics SCHAKAL.[26] CCDC reference number 631604. For crystallographic data in CIF or other electronic format see DOI: 10.1039/b705090a

Acknowledgements

Financial support by the Deutsche Forschungsgemeinschaft (Schwerpunktprogramm 1166 and Graduiertenkolleg 440) is gratefully acknowledged.

References

1 (*a*) D. Parker, *Chem. Ber.*, 1994, 833; (*b*) G. Mathis, *Clin. Chem. (Washington, D. C.)*, 1995, **41**, 1391; (*c*) V. Alexander, *Chem. Rev.*, 1995, **95**, 273; (*d*) D. Parker and J. A. G. Williams, *J. Chem. Soc., Dalton Trans.*, 1996, 3613; (*e*) J.-C. G. Bünzli and C. Piguet, *Chem. Rev.*, 2002, **102**, 1897; (*f*) D. Parker, R. S. Dickins, H. Puschmann, C. Crossland and J. A. K. Howard, *Chem. Rev.*, 2002, **102**, 1977. For selected recent examples see: ; (*g*) L. J. Charbonniere, R. Schurhammer, S. Mameri, G. Wipff and R. F. Ziessel, *Inorg. Chem.*, 2005, **44**, 7151; (*h*) S. Sivakumar, F. C. J. M. Van Veggel and M. Raudsepp, *J. Am. Chem. Soc.*, 2005, **127**, 12464.
2 C. Piguet and J.-C. G. Bünzli, *Chem. Soc. Rev.*, 1999, **28**, 347.
3 (*a*) S. I. Weissman, *J. Chem. Phys.*, 1942, **10**, 214; (*b*) G. A. Crosby, R. E. Whan and R. M. Alire, *J. Chem. Phys.*, 1961, **34**, 743; (*c*) G. A. Crosby, R. E. Whan and J. J. Freeman, *J. Am. Chem. Soc.*, 1962, **66**, 2493; (*d*) R. E. Whan and G. A. Crosby, *J. Mol. Spectrosc.*, 1962, **8**, 315. For a more recent review on the properties of lanthanides see: ; (*e*) J.-C. G. Bünzli, *Acc. Chem. Res.*, 2006, **39**, 53.

4 (*a*) J.-M. Lehn, *Supramolecular Chemistry*, VCH, Weinheim, 1995; (*b*) B. Alpha, J.-M. Lehn and G. Mathis, *Angew. Chem.*, 1987, **99**, 259 (*Angew. Chem., Int. Ed.*, 1987, **26**, 266).
5 A. P. Bassett, S. W. Magennis, P. B. Glover, D. J. Lewis, N. Spencer, S. Parsons, R. M. Williams, L. De Cola and Z. Pikramenou, *J. Am. Chem. Soc.*, 2004, **126**, 9413.
6 (*a*) K. Binnemans, Rare-earth Beta-diketonates, in *Handbook on the Physics and Chemistry of Rare Earths*, ed. K. A. Gschneidner, Jr, J.-C. G. Bünzli and V. K. Pecharsky, Elsevier, Amsterdam, 2005, vol. 35, ch. 225, pp. 107–272; see also ; (*b*) M. M. Castaño-Briones, A. P. Bassett, L. L. Meason, P. R. Ashton and Z. Pikramenou, *Chem. Commun.*, 2004, 2832; (*c*) S. V. Eliseeva, M. Ryazanov, F. Gumy, S. I. Troyanov, L. S. Lepnev, J.-C. G. Bünzli and N. P. Kuzmina, *Eur. J. Inorg. Chem.*, 2006, 4809.
7 For reviews on helicates see: (*a*) C. Piguet, G. Bernardinelli and G. Hopfgartner, *Chem. Rev.*, 1997, **97**, 2005; (*b*) M. Albrecht, *Chem. Rev.*, 2001, **101**, 3457; (*c*) M. J. Hannon and L. J. Childs, *Supramol. Chem.*, 2004, **16**, 7; (*d*) M. Albrecht, I. Janser and R. Fröhlich, *Chem. Commun.*, 2005, 157; (*e*) C. Piguet, M. Borkovec, J. Hamacek and K. Zeckert, *Coord. Chem. Rev.*, 2005, **249**, 705.
8 M. Albrecht, I. Janser, J. Fleischhauer, Y. Wang, G. Raabe and R. Fröhlich, *Mendeleev Commun.*, 2004, 250.
9 (*a*) M. Albrecht, S. Schmid, M. deGroot, P. Weis and R. Fröhlich, *Chem. Commun.*, 2003, 2526. For related complexes of β-diketonate ligands see: ; (*b*) R. W. Saalfrank, H. Maid, N. Mooren and F. Hampel, *Angew. Chem.*, 2002, **114**, 323 (*Angew. Chem., Int. Ed.*, 2002, **41**, 304); (*c*) V. A. Grillo, E. J. Seddon, C. M. Grant, G. Aromi, J. C. Bollinger, K. Folting and G. Christou, *Chem. Commun.*, 1997, 1561; (*d*) R. W. Saalfrank, V. Seitz, D. Caulder, K. N. Raymond, M. Teichert and D. Stalke, *Eur. J. Inorg. Chem.*, 1998, 1313; (*e*) D. E. Fenton, C. M. Regan, U. Casellato, P. A. Vigato and M. Vidali, *Inorg. Chim. Acta*, 1980, **44**, L105; (*f*) D. E. Fenton, C. M. Regan, U. Casellato, P. A. Vigato and M. Vidali, *Inorg. Chim. Acta*, 1982, **58**, 83; (*g*) M. M. Matsushita, T. Yasuda, R. Kawano, T. Kawai and T. Iyoda, *Chem. Lett.*, 2000, 812; (*h*) G. Aromi, C. Boldron, P. Gamez, O. Roubeau, H. Kooijman, A. L. Spek, H. Stoeckli-Evans, J. Ribas and J. Reedijk, *Dalton Trans.*, 2004, 3586; (*i*) J. K. Clegg, L. F. Lindoy, J. C. McMurtrie and D. Schilter, *Dalton Trans.*, 2005, 857.
10 For achiral helicates with lanthanides see: (*a*) C. Piguet, J.-C. G. Bünzli, G. Bernardinelli, G. Hopfgartner, S. Petoud and O. Schaad, *J. Am. Chem. Soc.*, 1996, **118**, 6681; (*b*) C. Edder, C. Piguet, J.-C. G. Bünzli and G. Hopfgartner, *J. Chem. Soc., Dalton Trans.*, 1997, 4657; (*c*) N. Martin, J.-C. G. Bünzli, V. McKee, C. Piguet and G. Hopfgartner, *Inorg. Chem.*, 1998, **37**, 577; (*d*) M. Elhabiri, R. Scopelliti, J.-C. G. Bünzli and C. Piguet, *J. Am. Chem. Soc.*, 1999, **121**, 10747; (*e*) F. R. Gonçalves e Silva, O. L. Malta, C. Reinhard, H.-U. Güdel, C. Piguet, J. E. Moser and J.-C. G. Bünzli, *J. Phys. Chem. A*, 2002, **106**, 1670.
11 J. J. Lessmann and W. D. Horrocks, *Inorg. Chem.*, 2000, **39**, 3114.
12 For example:(*a*) M. Cantuel, G. Bernardinelli, G. Muller, J. P. Riehl and C. Piguet, *Inorg. Chem.*, 2004, **43**, 1840; (*b*) D. Parker, *Chem. Soc. Rev.*, 2004, **33**, 156.
13 For example: (*a*) O. Mamula, M. Lama, S. G. Telfer, A. Nakamura, R. Kuroda, H. Stoeckli-Evans and R. Scopelitti, *Angew. Chem.*, 2005, **117**, 2583 (*Angew. Chem., Int. Ed.*, 2005, **44**, 2527); (*b*) O. Mamula, M. Lama, H. Stoeckli-Evans and S. Shova, *Angew. Chem.*, 2006, **118**, 5062–5066 (*Angew. Chem., Int. Ed.*, 2006, **45**, 4940).
14 M. Albrecht, S. Dehn, S. Schmid and M. de Groot, *Synthesis*, 2007, 155.
15 (*a*) G. Urbain, *C. R. Hebd. Seances Acad. Sci.*, 1897, **124**, 618; (*b*) J. A. Cunningham, D. E. Sands and W. F. Wanger, *Inorg. Chem.*, 1967, **6**, 499; (*c*) T. Philips, D. E. Sands and W. F. Wagner, *Inorg. Chem.*, 1968, **7**, 2295.
16 M. Albrecht, S. Dehn, G. Raabe and R. Fröhlich, *Chem. Commun.*, 2005, 5690.
17 (*a*) N. Filipescu, M. R. Kagan, N. McAvoy and F.A. Serafin, *Nature*, 1962, **196**, 467; (*b*) N. Filipescu, W. F. Sager and F. A. Serafin, *J. Phys. Chem.*, 1964, **68**, 3324; (*c*) W. F. Sager, N. Filipescu and F. A. Serafin, *J. Phys. Chem.*, 1965, **69**, 1092; (*d*) G. H. Dieke *Spectra and Energy Levels of Rare Earth Ions in Crystals*, Interscience Publishers, New York, 1968.
18 C. Görller-Walrand and K. Binnemans, *Rationalization of Crystal-Field Parametrization*, in *Handbook on the Physics and Chemistry of Rare Earths*, ed. K. A. Gschneidner, Jr, J.-C. G. Bünzli and V. K. Pecharsky, Elsevier, Amsterdam, 1996, vol. 23, ch. 155.
19 E. Nakazawa and S. Shionoya, *J. Phys. Soc. Jpn.*, 1970, **28**, 1260.
20 (*a*) H. B. Bauer and D. L. Ross, *J. Am. Chem. Soc.*, 1965, **86**, 5125; (*b*) W. D. Horrocks, Jr and M. Albin, *Prog. Inorg. Chem.*, 1983, **31**, 1.
21 For a recent example of a quadruple-stranded helicate see: J. Xu and K. N. Raymond, *Angew. Chem.*, 2006, **118**, 6630–6635 (*Angew. Chem., Int. Ed.*, 2006, **45**, 6480).
22 S. W. Magennis, S. Parsons and Z. Pikramenou, *Chem.–Eur. J.*, 2002, **8**, 5761.
23 Z. Otwinowski and W. Minor, *Methods Enzymol.*, 1997, **276**, 307.
24 Z. Otwinowski, D. Borek, W. Majewski and W. Minor, *Acta Crystallogr., Sect. A: Found. Crystallogr.*, 2003, **A59**, 228.
25 G. M. Sheldrick, *SHELXS-97, Program for solution of crystal structures*, University of Göttingen, Germany, 1997G. M. Sheldrick, *SHELXL-97, Program for refinement of crystal structures*, University of Göttingen, Germany, 1997.
26 E. Keller, *SCHAKAL*, Universität Freiburg, Germany, 1997.

